Effects of Y doping on the structural stability and defect properties of cubic HfO_2

G. H. Chen,[1] Z. F. Hou,[1] X. G. Gong,[1,a)] and Quan Li[2]
[1]*Surface Physics Laboratory (National Key) and Department of Physics, Fudan University, Shanghai 200433, People's Republic of China*
[2]*Department of Physics, The Chinese University of Hong Kong, Shatin, New Territory, Hong Kong*

(Received 16 May 2008; accepted 31 July 2008; published online 1 October 2008)

First-principles calculations have been performed to study the structural and electronic properties of pure and Y-doped cubic HfO_2. It is found that Y doping in HfO_2 would increase the stability of the cubic phase relative to the monoclinic phase by reducing the energy difference and the phase transition pressure. This result is consistent with the observed stabilization of the cubic phase of HfO_2 by the addition of Y. The calculated formation energy of the V_O-Y_{Hf} complex defect in different charged states indicates that the single positively charged state $(V_O-Y_{Hf})^+$ is more stable than the neutral state $(V_O-Y_{Hf})^0$ and the double positively charged state $(V_O-Y_{Hf})^{++}$ in Y-doped cubic HfO_2. Because the number of *d*-electrons of Y is less than that of Hf by one and substitutional Y for Hf introduces holes in the oxygen *p*-band, Y doping would make the highest occupied defect level induced by $(V_O-Y_{Hf})^+$ fall into the valence band rather than the energy gap, which explains the experimental observation that gap states related to oxygen vacancy defects become nondetectable in Y-doped HfO_2 films. © *2008 American Institute of Physics*. [DOI: 10.1063/1.2985908]

I. INTRODUCTION

The progressive down-scaling process of Si-based complementary metal-oxide-semiconductor devices particularly results in a requirement of wide band gap insulating metal oxides with high dielectric constant (high-κ) to replace the conventional silicon dioxide (SiO_2) gate oxide films, in order to reduce leakage current and achieve the desired device area while maintaining the gate capacitance.[1–3] Among the possible candidates, HfO_2 is one of the most attractive dielectrics due to its high dielectric constant of 25,[2] reasonable band gap offsets with silicon,[4,5] and thermodynamical stability on Si substrate.[6]

At atmospheric pressure HfO_2 exists in three structures, i.e., monoclinic, tetragonal, and cubic phases, and the thermodynamic stability of each phase strongly depends on temperature.[7] Only the monoclinic phase of HfO_2 is stable at low temperatures, the stabilization of tetragonal phase of HfO_2 requires significantly higher temperature (above 2000 K), and cubic phase of HfO_2 becomes stable even above 2870 K. First-principles study[8] has predicted that HfO_2 exhibits higher permittivity, κ, in the cubic ($\kappa \sim 29$) or in the tetragonal ($\kappa \sim 70$) structure than in the monoclinic one ($\kappa \sim 16-18$). Therefore it is desirable to prepare HfO_2 in the cubic or tetragonal form at lower temperature, even at room temperature.[9] In view of the fact that the cubic phase of HfO_2 crystallizes in a fluorite-type structure and Y_2O_3 in a body-centered cubic structure, the close correlation between these two structures[10] gives the possibility that addition of Y_2O_3 would stabilize the cubic structure of HfO_2 at lower temperature. Early experimental studies[11–13] showed that solid solution of HfO_2 and Y_2O_3 can be stabilized in cubic form for the atomic percentage (at. %) of Y from 8/15 at. % up to 50/60 at. % at temperatures as low as 1500 °C. The stabilization of cubic HfO_2 for lower Y concentration (~6.5 at. % and ~4 at. %, $(HfO_2)_{0.9}$-$(Y_2O_3)_{0.1}$, and $(HfO_2)_{0.8}$-$(Y_2O_3)_{0.2}$), was also observed recently[9,14–16] by x-ray diffraction and transmission electron microscopy. It was also found that the incorporated Y atom substitutes for Hf in the crystalline lattice homogeneously.[17] Although these experiments demonstrated the phase transition of HfO_2 induced by addition of Y_2O_3, the driving mechanism for stabilizing the cubic structure of Y-doped HfO_2 is not clear yet. Understanding the effect of Y doping on the stability of cubic HfO_2 at atomic scale is desirable.

Recently oxygen vacancies in HfO_2 have attracted much attention because this type of defects is probably one kind of the major traps contributing to charge trapping in HfO_2 (Refs. 18 and 19) and severely affects the electrical behavior of the dielectric films, such as leakage current and charge scattering.[20] Oxygen vacancies in HfO_2 have been theoretically predicted by *ab initio* calculations[21,22] and observed experimentally as well.[23–25] The removal of oxygen vacancies in HfO_2 has become a major issue for its device application. Recent studies demonstrated that doping third elements such as Al,[25] N,[26,27] and F (Ref. 28) into HfO_2 could passivate the oxygen vacancies. The electronic structure calculations on density of states (DOS) of ZrO_2 with structure similar to that of HfO_2 indicate that oxygen vacancy in ZrO_2 induces gap states, but no gap states result from the complex defect consisting of impurity Y and oxygen vacancy.[29] The x-ray photoelectron spectroscopy (XPS) spectra of HfO_2 films with and without addition of Y_2O_3 demonstrated that in the pure HfO_2 films some occupied states are located between the Fermi level and the valence band maximum, but

a)Electronic mail: xggong@fudan.edu.cn.

such occupied states have not been detected in the Y-doped HfO_2 films.[16] These occupied states in XPS spectrum of pure HfO_2 are attributed to the oxygen-vacancy-related defects,[25] suggesting that doping Y into HfO_2 could also passivate the oxygen vacancies. This motivates us to conduct *ab initio* simulations in order to show the effect of Y doping on electronic structures of oxygen vacancies in HfO_2.

In this work, we have conducted a comprehensive theoretical study on the structural stability of monoclinic and cubic phases of HfO_2 with and without dopant Y, and on the electronic structures of oxygen vacancies and complex defects formed by oxygen vacancy with Y substitution for Hf in cubic HfO_2. All calculations presented are carried out by the plane wave pseudopotential method within the generalized gradient approximation (GGA). The rest of this paper is organized as follows: In Sec. II we present the details of the calculations. In Sec. III we discuss the results for structural stability of monoclinic and cubic phases of pure and Y-doped HfO_2, and electronic structures of oxygen vacancies in cubic HfO_2 with and without Y substitution. Section IV summarizes the work.

II. COMPUTATIONAL METHOD

All calculations are performed by using the plane wave pseudopotential methods within density functional theory,[30] as implemented in the VASP code.[31,32] The ultrasoft pseudopotentials are employed to represent the interactions between the ion core and the valence electrons.[33] The exchange correlation functional is treated within the GGA of Perdew and Wang.[34] Wave functions are expanded in a plane wave basis set with cutoff energy (E_{cut}) 495 eV. For structure optimization, conjugate gradient method is used for the relaxation of atoms until the residual forces are less than 0.01 eV/Å. The k-points in the Brillouin zone (BZ) are generated by the Monkhorst–Pack scheme for BZ integrations. Tests on k-point sampling have been done to make sure that the total energies are converged.

A. Bulk calculations and equation of state

As a starting point for our investigation we have carried out the calculations of monoclinic and cubic phases of pure bulk HfO_2 to determine the structural parameters. We conduct the structural optimization for the monoclinic and cubic phases of HfO_2, starting from experimentally reported geometry.[12,35,36] For each phase, we calculate the total energies for many different cell volumes. For each given volume, we optimize all the lattice parameters and relax internal parameters using the conjugate gradient method. The obtained energies are fitted with the Birch–Murnaghan equation of state[37] to give the equilibrium volume and the minimum energy. The $9\times9\times9$ and $5\times5\times5$ k-point meshes are used in BZ integrations for the calculations of cubic and monoclinic phases of pure HfO_2, respectively.

In order to study the effect of Y doping on structural stability of HfO_2, we also perform the structural optimization of Y-doped monoclinic and cubic HfO_2 with the Y content at Y:Hf=1:7 (12.5 mol % yttrium) in the above manner. In this case, the Y-doped HfO_2 is modeled by one HfO_2 supercell containing 24 atoms, which is generated by $1\times1\times2$ extending the primitive cell of monoclinic HfO_2 and $2\times2\times2$ for cubic HfO_2. In the present paper, we focus the calculation only on the substitution of Y for Hf, compatible with the experimental study.[17] The $5\times5\times5$ and $5\times5\times3$ k-point meshes are used in BZ integrations for the calculations of cubic and monoclinic phases of Y-doped HfO_2, respectively.

B. Defect formation energies

For all the further investigations on defects we increase the supercell size of cubic HfO_2, so that small amounts of Y impurities and/or oxygen vacancies can be examined. Therefore, a $3\times3\times3$ supercell containing 27 HfO_2 formula units is used for studying the defects in cubic HfO_2. With this setup, the available minimum of Y content is Y:Hf=1:26 (3.7 mol % yttrium). The substitution of Y for Hf (Y_{Hf}) is realized by replacing one of the lattice Hf atoms with a Y atom in the relaxed cubic HfO_2 supercell. To introduce an isolated oxygen vacancy (V_O), one interior oxygen atom is removed from the supercell. The V_O-Y_{Hf} complex defect is formed by an oxygen vacancy and one substitutional Y on Hf site. A neutralizing background charge is applied to the supercell for the calculations of charged defects.

The formation energy of point defect in cubic HfO_2 is calculated from the total energy of defective supercell according to the standard formalism.[38–40] For a defect α in charge state q in the cubic HfO_2, its formation energy is a function of both the Fermi level ε_F and the chemical potentials of Hf, O, and Y (μ_{Hf}, μ_Y, μ_O) involved in the defect:

$$E_f(\alpha,q) = E(\alpha,q) - (E_0^0 + n_{Hf}\mu_{Hf} + n_O\mu_O + n_Y\mu_Y) + q(\varepsilon_F + E_{VBM}), \quad (1)$$

where $E(\alpha,q)$ is the total energy of the defective supercell, E_0^0 is the total energy of the perfect HfO_2 supercell, and n_{Hf}, n_O, and n_Y are the numbers of Hf, O, and Y atoms removed and/or added to the perfect supercell to introduce an oxygen vacancy or Y substitution on Hf site. For example, $n_{Hf}=-1$, $n_Y=1$ and $n_O=-1$ stands for a complex defect of V_O-Y_{Hf}. The Fermi level ε_F is measured relative to the valence band maximum (VBM), E_{VBM}. With periodic boundary conditions the potential is determined only up to a constant; in order to accurately determine the E_{VBM} it is necessary to line up the potential of the perfect supercell with that of the defective one. For this purpose, the average electrostatic potentials of the atoms far away from the defect in the defective supercell are aligned with those of the corresponding atoms in the perfect supercell.[41] As for the oxygen vacancy and the complex defect of V_O-Y_{Hf}, their charge q varying from neutral to fully ionized states (i.e., $0\sim+2$) are considered.

In order to study the stable charged defect states and the possible role that defects play in photo-stimulated processes, we consider the ionization energies of defect states with respect to the bottom of the conduction band of cubic HfO_2, following the studies on oxygen vacancies and interstitials in monoclinic HfO_2.[21] We calculate the defect ionization energy $I_p(\alpha,q)$ defined as the vertical excitation energy of an electron from the defect with charge q to the bottom of the conduction band,[21] i.e.,

TABLE I. Calculated structural parameters of the monoclinic and cubic phases of HfO_2. V_0 (in $Å^3$ per formula HfO_2) is the equilibrium volume, a, b, and c (in Å) are the lattice constants, β (in degree) is the angle between lattice vector $\vec{a}$ and $\vec{c}$, and B_0 (in GPa) is the bulk modulus.

	Present work	Other work[a]		Expt.[b]
Monoclinic				
V_0	34.73	36.39	34.81	34.62
a	5.130	5.215	5.132	5.119
b	5.187	5.293	5.189	5.170
c	5.298	5.350	5.307	5.298
β	99.77	99.73	99.78	99.18
B_0	179	192		185
Cubic				
V_0	32.43	34.10	32.49	32.77
a	5.06	5.148	5.07	5.08
B_0	261	257		

[a]References 21 and 44.
[b]References 12, 35, and 36.

$$I_p(\alpha,q) = E_0^- + E_\alpha^{q+1} - E_0^0 - E_\alpha^q + \xi, \quad (2)$$

where E_0^{-1} and E_0^0 are the calculated energies of perfect supercell with charge −1 and 0, respectively. E_α^q is the energy of the defective supercell containing defect α with charge q. Note that the E_α^{q+1} is calculated with the geometry of the relaxed defective supercell containing defect α with charge q. Due to the band gap or conduction band edge underestimated in GGA calculations, ξ is taken for correction of the conduction band minimum and defined as the difference between experimental band gap value (E_g^{expt}) and theoretically calculated one (E_g^{theor}). This approximation is the main source of inaccuracy for the defect levels. Here $E_g^{\text{expt}} = 5.68$ eV (Ref. 42) is used and E_g^{theor} can be obtained by following the formula,[43]

$$E_g^{\text{theor}} = E_0^- + E_0^+ - 2 * E_0^0, \quad (3)$$

and the band gap calculated is about 4.06 eV, which is smaller than the experimental value of 5.68 eV.[42]

III. RESULTS AND DISCUSSIONS

A. Structure and relative stability

The calculated lattice parameters (a, b, c and β), equilibrium volume V_0, and bulk modulus B_0 of monoclinic and cubic phases of HfO_2 are all listed in Table I, along with experimental data and other theoretical results for comparison. For both monoclinic and cubic phases of HfO_2, we have found good agreements between calculated and available experimental values[12,35,36] of structural parameters. The results are also consistent with previous GGA calculations[21,44] and experimental observation.[12]

The calculated total energies of monoclinic and cubic phases of HfO_2 are plotted as a function of volume, as shown in Fig. 1. The energy difference between cubic and monoclinic phases at equilibrium is 238 meV, which agrees well with another calculated result[21] (240 meV). The total energies versus volumes for Y-doped monoclinic and cubic HfO_2 with Y:Hf=1:7 are also shown in Fig. 1. For this concentration of dopant Y in HfO_2, the calculated total energies

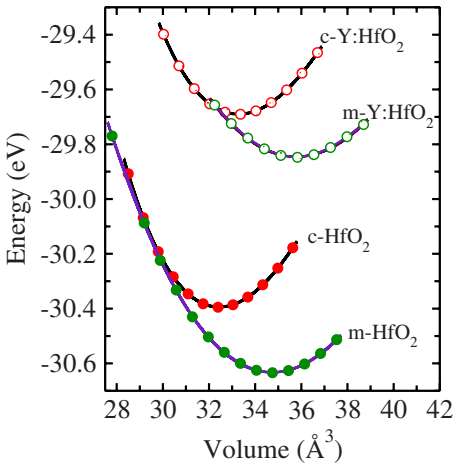

FIG. 1. (Color online) Calculated cohesive energy versus volume (per HfO_2 formula unit) for cubic (c) and monoclinic (m) phases of HfO_2 and Y-doped HfO_2 (Y:HfO_2).

indicate that the monoclinic phase is still energetically more stable than the cubic phase, but the energy difference between monoclinic and cubic phases of Y-doped HfO_2 is greatly decreased to 135 meV. Generally, the free energy $G = E + PV - TS$ should be used to determine the most stable structure at finite pressure and temperature. However present work focuses on the physics properties of materials at 0 K, therefore we neglect the last term and work with the enthalpy $H = E + PV$. The transition pressure between two phases can be estimated by the crossing point of their enthalpies. The relative enthalpy of cubic phase with respect to monoclinic phase as a function of pressure is shown in Fig. 2. As shown

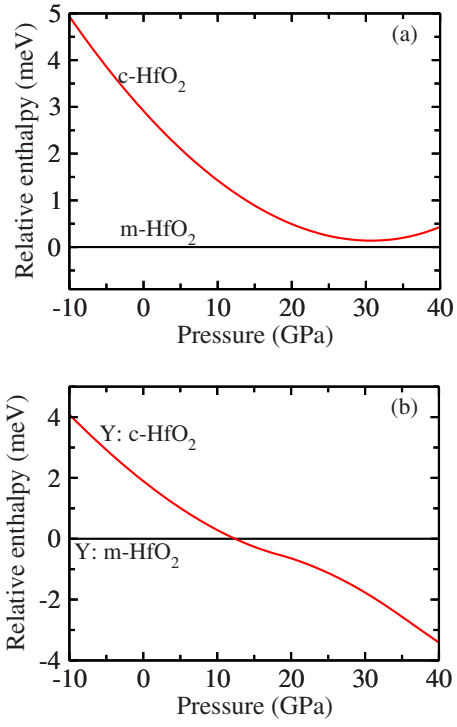

FIG. 2. (Color online) Calculated enthalpy versus pressure (per HfO_2 formula unit) for cubic (c) and monoclinic (m) phases of HfO_2 and Y-doped HfO_2 (Y:HfO_2). The data is presented with respect to that of monoclinic phase.

TABLE II. Total energies of defective supercells containing V_O-Y_{Hf} complex at different charge state (q) with different nearest-neighbor distance (NND) between V_O and Y_{Hf}. The values (in eV) listed are relative to those of the second NND.

q	First NND	Second NND	Third NND	Fourth NND
0	0.201	0	0.176	0.131
+	0.504	0	0.325	0.223
++	0.486	0	0.289	0.183

in Fig. 2(a), there is no crossing between monoclinic and cubic phases for pure HfO_2, implying that pressure-induced monoclinic to cubic transition is impossible at zero temperature. For the monoclinic and cubic phases of Y-doped HfO_2, the transition pressure from monoclinic to cubic phases is about 12.4 GPa, as shown in Fig. 2(b). The phase-diagram of HfO_2 indicates that phase transition between monoclinic and cubic structures of HfO_2 is mostly caused by the thermal treatment at high temperature and cubic phase of pure HfO_2 becomes stable above 2870 K.[7] The transition induced by pressure at zero temperature and the decrease in energy difference between monoclinic and cubic phase suggest Y addition into HfO_2 would lower the transition temperature. Recent experiment[9] has demonstrated that a pure cubic phase of HfO_2 is stabilized with Y content of 6.5 at. % and the cubic phase is stable upon high temperature rapid thermal annealing at 900 °C under NH_3. All of these results indicate that Y doping in HfO_2 enhances the stability of cubic phase by decreasing the energy difference and reducing the transition pressure.

B. Oxygen vacancies with dopant Y in cubic HfO_2

In order to study the effect of Y doping on oxygen vacancies (V_O) in cubic HfO_2, V_O in pure and Y-doped cubic HfO_2 are both investigated. Especially for the case of Y-doped HfO_2, we first consider the interaction between Y substitution on Hf site (Y_{Hf}) and V_O. The energy differences of defective supercells containing V_O-Y_{Hf} complex defect with different charge states and with different distances between V_O and Y_{Hf} are listed in Table II. It can be seen that the system studied is energetically favorable when the V_O is the second nearest neighbor of the Y_{Hf}, which is consistent with the results of the first-principles studies on oxygen vacancies in Y-doped cubic and tetragonal ZrO_2.[29,45] Therefore in the following sections, we only focus on the case of V_O-Y_{Hf} complex formed by V_O and Y_{Hf} as its second nearest neighbor.

Considering that oxygen vacancies are usually detected in insufficiently oxidized hafnia films containing less oxygen than stoichiometric HfO_2,[24] the calculated formation energies of V_O and V_O-Y_{Hf} in cubic HfO_2 under oxygen-deficient condition are listed in Table III. A negative formation energy indicates that the system is stable with respect to the chemical potential (growth condition). The oxygen deficiency in cubic HfO_2 corresponds to that of the chemical potential of oxygen which is defined as

TABLE III. Defect formation energies E_f (in eV) of V_O point defect and V_O-Y_{Hf} complex defect in cubic HfO_2 under oxygen-deficient condition ($\mu_O=\mu_O^0+\frac{1}{2}\Delta E_f^{HfO_2}$). ε_F is measured relative to the VBM of HfO_2, and 3.68 eV is the calculated value of the band gap.

Defect	E_f	
	$\varepsilon_F=0$ eV	$\varepsilon_F=3.68$ eV
V_O^0	0.78	0.78
V_O^+	−2.18	1.50
V_O^{++}	−6.25	1.11
$(V_O-Y_{Hf})^0$	−0.86	−0.86
$(V_O-Y_{Hf})^+$	−4.93	−1.25
$(V_O-Y_{Hf})^{++}$	−4.89	2.47

$$\mu_O = \mu_O^0 + \frac{1}{2}\Delta E_f^{HfO_2}, \tag{4}$$

where $\Delta E_f^{HfO_2}$ is the heat of formation energy of cubic HfO_2. The calculated formation energy of neutral V_O in cubic HfO_2 is 0.78 eV while the defect formation energy of neutral V_O-Y_{Hf} is about −0.86 eV, which is lower than that of neutral V_O because Y and O prefer to form stoichiometric Y_2O_3. In order to study the stability of V_O and V_O-Y_{Hf} in a range of charged states, we consider their formation energies versus the Fermi levels. As shown in Fig. 3, the lower limit of the Fermi level ($\varepsilon_F=0$ eV) corresponds to the top of the valence band while the upper limit ($\varepsilon_F=3.68$ eV) represents the bottom of the calculated conduction band. The slope of the line in Fig. 3 corresponds to the charge state of the defect. Oxygen vacancy in the double positively charged state (V_O^{++}) is more stable than single positively charged oxygen vacancy (V_O^+) for a wide range of Fermi levels. Also, only for Fermi levels close to the conduction band neutral V_O is the lowest in energy, while V_O-Y_{Hf} complex defect is stable in

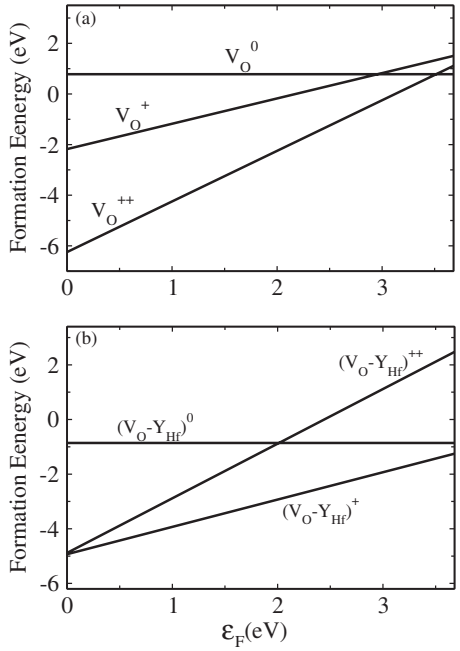

FIG. 3. Calculated defect formation energy of V_O point defect and V_O-Y_{Hf} complex defect in cubic HfO_2 as a function of Fermi energy under oxygen-deficient condition ($\mu_O=\mu_O^0+\frac{1}{2}\Delta E_f^{HfO_2}$).

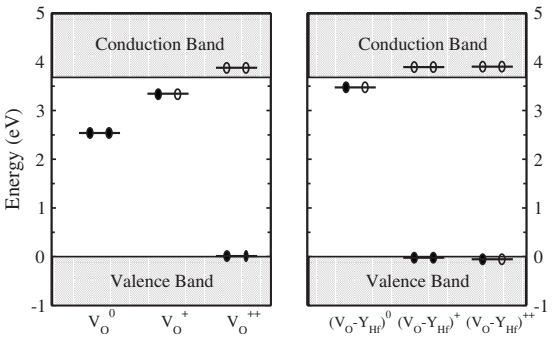

FIG. 4. Schematic representation of the single-electron energy levels in the calculated band gap of cubic HfO_2 induced by V_O point defect and V_O-Y_{Hf} complex defect in different charged states. The solid and open circles indicate occupied and unoccupied states, respectively.

single positively charged state rather than double positively charged state for all Fermi levels. These are understandable because the reaction of $V_O^{++}+V_O^0 \rightarrow 2V_O^+$ is endothermic and the energy required is about 1.11 eV, which is consistent with previous calculated results,[46] while the reaction of $(V_O-Y_{Hf})^{++}+(V_O-Y_{Hf})^0 \rightarrow 2(V_O-Y_{Hf})^+$ releases an energy of 4.12 eV. Above results indicate that once V_O interacts with its second nearest Y_{Hf}, the oxygen vacancy prefers to be in a single positively charged state.

The schematic representation of the single-electron energy levels in the calculated band gap of cubic HfO_2 induced by V_O and complex defect V_O-Y_{Hf} are shown in Fig. 4. It can be seen that the formation of neutral V_O introduces a fully occupied defect state at 2.54 eV above the VBM of HfO_2. In our previous work on Al-incorporated HfO_2 films,[25] occupied DOS peaked at ~2.5 eV above the VBM are detected in the XPS spectrum of pure HfO_2 films, and such DOS are commonly attributed to the oxygen-vacancy-related defects.[18,23] The corresponding vertical ionization energy is about 3.69 eV (see Fig. 5). For V_O^+, its highest occupied level with one electron is located at 3.35 eV, and the vertical ionization energy of V_O^+ is about 2.78 eV. V_O^{++} induces a fully unoccupied defect level at 3.88 eV above VBM. Because GGA underestimates the band gap of cubic HfO_2, this level is located within the calculated conduction bands. Once V_O interacts with its second nearest Y_{Hf}, complex defect V_O-Y_{Hf} forms. Consequently, the fully occupied defect level induced by V_O^0 moves to 3.47 eV and it turns to be occupied by one electron in the case of $(V_O-Y_{Hf})^0$. The vertical ionization energy of $(V_O-Y_{Hf})^0$ is about 2.72 eV. For $(V_O-Y_{Hf})^+$, its highest occupied level with two electrons is located in the vicinity of the VBM and the lowest unoccupied level appears at 3.89 eV above VBM, i.e., appearing within the calculated conduction bands, which corresponds to the defect level induced by V_O^{++}. For $(V_O-Y_{Hf})^{++}$, its highest occupied level with one electron appears in the vicinity of the VBM and the lowest unoccupied level is located at 3.90 eV above VBM. Because the position of the highest occupied level of both $(V_O-Y_{Hf})^+$ and $(V_O-Y_{Hf})^{++}$ is located in the vicinity of the VBM, their corresponding vertical ionization energies are 5.96 eV and 6.09 eV, respectively. In experiment, no defect DOS above the VBM is detected in the XPS spectrum of Y-doped HfO_2 film with the Hf:Y ratio of about 9:1.[16] From the theoretically determined highest occupied defect states induced by V_O and its corresponding ionization energy, the neutral V_O and charged V_O^+ may contribute to the detected defect DOS in pure HfO_2.[16,25] Once one of lattice Hf atoms near V_O is substituted by one Y atom, the highest fully occupied defect level due to neutral V_O would turn to be occupied by one electron and highest occupied defect level induced by V_O^+ lowers into valence bands. This can be seen from the single-electron energy levels in the calculated band gap induced by $(V_O-Y_{Hf})^0$ and $(V_O-Y_{Hf})^+$. Considering that Y and Hf are not isovalent, Y possesses *d*-electrons less than Hf by one, and Y_{Hf} just makes the oxygen *p*-band no longer fully occupied,[29] it could be expected that if more than one of lattice Hf atoms are substituted by Y atoms, the highest fully occupied defect level due to neutral V_O could also fall into the valence band. These results suggest that the passivation of the defect states related to oxygen vacancies by dopant Y contributes to the evolution of defect DOS observed in XPS spectra of the pure HfO_2 and the Y-incorporated HfO_2 thin films.[16]

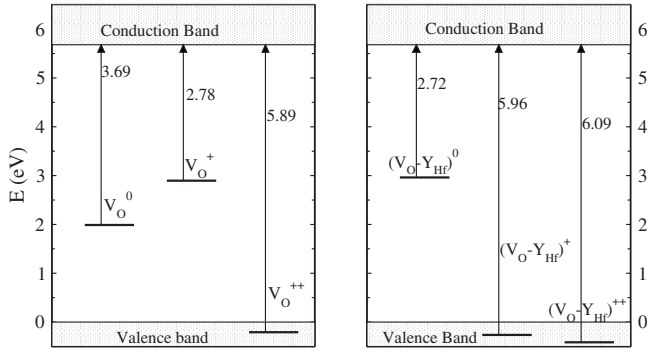

FIG. 5. Defect ionization energies of V_O point defect and V_O-Y_{Hf} complex defect in different charged states.

IV. CONCLUSIONS

We have performed first-principles calculations to investigate the effects of Y doping on the structural stability of HfO_2 and electronic structures of oxygen vacancies in cubic HfO_2. The results suggest that the stabilization of cubic phase of Y-doped HfO_2 could be understood from the point of view that doping Y into HfO_2 decreases the energy difference between the cubic phase and the monoclinic phase and enhances the possibility of pressure-induced phase transition as well. The results of electronic structure of oxygen vacancies in HfO_2 and Y-doped HfO_2 indicate that dopant Y changes the charge state of oxygen vacancy, and most importantly, it passivates the gap states induced by oxygen vacancies, which also explains the observed evolution of the occupied density of states between Fermi level and valence band maximum in HfO_2 films upon Y addition.

ACKNOWLEDGMENTS

X.G.G. was partially supported by the NSF of China, the national program for the basic research and research project of Shanghai. Z.F.H. acknowledges support from NSF of China under Grant No. 10674028 and Shanghai Postdoctoral Science Foundation under Grant No. 05R214106. Q.L. ac-

knowledges the RGC grant under Project No. CUHK402105. The computation was performed at Shanghai Supercomputer Center and Supercomputer Center of Fudan University and CCS.

[1]P. A. Packan, Science **285**, 2079 (1999).
[2]G. D. Wilk, R. M. Wallace, and J. M. Anthony, J. Appl. Phys. **89**, 5243 (2001).
[3]A. I. Kingon, J. P. Maria, and S. K. Streiffer, Nature (London) **406**, 1032 (2000).
[4]Y.-S. Lin, R. Puthenkovilakam, and J. P. Chang, Appl. Phys. Lett. **81**, 2041 (2002).
[5]J. Robertson, J. Vac. Sci. Technol. B **18**, 1785 (2000).
[6]L. Kang, K. Onishi, Y. Jeon, B. H. Lee, C. Kang, W.-J. Qi, R. Nieh, S. Gopalan, R. Choi, and J. C. Lee, Tech. Dig. - Int. Electron Devices Meet., **2000**, 35.
[7]O. Ohtaka, H. Fukui, T. Kunisada, T. Fujisawa, K. Funakoshi, W. Utsumi, T. Irifune, K. Kuroda, and T. Kikegawa, J. Am. Ceram. Soc. **84**, 1369 (2001).
[8]X. Zhao and D. Vanderbilt, Phys. Rev. B **65**, 233106 (2002).
[9]E. Rauwel, C. Dubourdieu, B. Holländer, N. Rochat, F. Ducroquet, M. D. Rossell, G. Van Tendeloo, and B. Pelissier, Appl. Phys. Lett. **89**, 012902 (2006).
[10]P. Duwez, F. H. Brown, Jr., and F. Odell, J. Electrochem. Soc. **98**, 356 (1951).
[11]D. W. Stacy and D. R. Wilder, J. Am. Ceram. Soc. **58**, 285 (1975).
[12]J. Wang, H. P. Li, and R. Stevens, J. Mater. Sci. **27**, 5397 (1992).
[13]M. Yashima, H. Takahashi, K. Ohtake, T. Hirose, M. Kakihana, H. Arashi, Y. Ikuma, Y. Suzuki, and M. Yoshimura, J. Phys. Chem. Solids **57**, 289 (1996).
[14]M. Komatsu, R. Yasuhara, H. Takahashi, S. Toyoda, H. Kumigashira, M. Oshima, D. Kukuruznyak, and T. Chikyow, Appl. Phys. Lett. **89**, 172107 (2006).
[15]K. Kita, K. Kyuno, and A. Toriumi, Appl. Phys. Lett. **86**, 102906 (2005).
[16]Q. Li and X. F. Wang (unpublished).
[17]Z. K. Yang, W. C. Lee, Y. J. Lee, P. Chang, M. L. Huang, M. Hong, K. L. Yu, M.-T. Tang, B.-H. Lin, C.-H. Hsu, and J. Kwo, Appl. Phys. Lett. **91**, 202909 (2007).
[18]H. Takeuchi, H. Y. Wong, D. Ha, and T.-J. King, Tech. Dig. - Int. Electron Devices Meet. **2004**, 829.
[19]S. Guha and V. Narayanan, Phys. Rev. Lett. **98**, 196101 (2007).
[20]K. Torii, A. Aoyama, S. Kamiyama, Y. Tamura, S. Miyazaki, H. Kitajima, and T. Arikado, Dig. Tech. Pap. - Symp. VLSI Technol., **2004**, 112.
[21]A. S. Foster, F. L. Gejo, A. L. Shluger, and R. M. Nieminen, Phys. Rev. B **65**, 174117 (2002).
[22]K. Xiong and J. Robertson, Microelectron. Eng. **80**, 408 (2005).
[23]A. Y. Kang, P. M. Lenahan, and J. F. Conley, Jr., Appl. Phys. Lett. **83**, 3407 (2003).
[24]H. Takeuchi, D. Ha, and T.-J. King, J. Vac. Sci. Technol. A **22**, 1337 (2004).
[25]Q. Li, K. M. Koo, W. M. Lau, P. F. Lee, J. Y. Dai, Z. F. Hou, and X. G. Gong, Appl. Phys. Lett. **88**, 182903 (2006).
[26]N. Umezawa, K. Shiraishi, T. Ohno, H. Watanabe, T. Chikyow, K. Torii, K. Yamabe, K. Yamada, H. Kitajima, and T. Arikado, Appl. Phys. Lett. **86**, 143507 (2005).
[27]K. Xiong, J. Robertson, and S. J. Clark, J. Appl. Phys. **99**, 044105 (2006).
[28]W. Chen, Q.-Q. Sun, S.-J. Ding, D. W. Zhang, and L.-K. Wang, Appl. Phys. Lett. **89**, 152904 (2006).
[29]A. Eichler, Phys. Rev. B **64**, 174103 (2001).
[30]W. Kohn and L. J. Sham, Phys. Rev. **140**, A1133 (1965).
[31]G. Kresse and J. Furthmüller, Comput. Mater. Sci. **6**, 15 (1996).
[32]G. Kresse and J. Furthmüller, Phys. Rev. B **54**, 11169 (1996).
[33]D. Vanderbilt, Phys. Rev. B **41**, 7892 (1990).
[34]J. P. Perdew, J. A. Chevary, S. H. Vosko, K. A. Jackson, M. R. Pederson, D. J. Singh, and C. Fiolhais, Phys. Rev. B **46**, 6671 (1992).
[35]D. M. Adams, S. Leonard, D. R. Russell, and R. J. Cernik, J. Phys. Chem. Solids **52**, 1181 (1991).
[36]D. W. Stacy, J. K. Johnstone, and D. R. Wilder, J. Am. Ceram. Soc. **55**, 482 (1972).
[37]F. Birch, Phys. Rev. **71**, 809 (1947).
[38]S. B. Zhang and J. E. Northrup, Phys. Rev. Lett. **67**, 2339 (1991).
[39]S.-H. Wei, Comput. Mater. Sci. **30**, 337 (2004).
[40]C. G. Van de Walle and J. Neugebauer, J. Appl. Phys. **95**, 3851 (2004).
[41]D. B. Laks, C. G. Van de Walle, G. F. Neumark, P. E. Blöchl, and S. T. Pantelides, Phys. Rev. B **45**, 10965 (1992).
[42]M. Balog, M. Schieber, M. Michman, and S. Patai, Thin Solid Films **41**, 247 (1977).
[43]S. T. Pantelides, D. J. Mickish, and A. B. Kunz, Phys. Rev. B **10**, 5203 (1974).
[44]J. Kang, E.-C. Lee, and K. J. Chang, Phys. Rev. B **68**, 054106 (2003).
[45]G. Stapper, M. Bernasconi, N. Nicoloso, and M. Parrinello, Phys. Rev. B **59**, 797 (1999).
[46]Y. P. Feng, A. T. L. Lim, and M. F. Li, Appl. Phys. Lett. **87**, 062105 (2005).